

Experimental investigation on validation of the mini wave gauge for ocean wave measurements in comparison to an acoustic doppler current profiler and HOBO

Rikha Widiaratih^{1,2*} , Ari Bawono Putranto³ , Lilik Maslukah¹ ,
Anindya Wirasatriya¹ , Eridhani Dharma Satya⁴ , Daenk Himawa¹ 

¹ Department of Oceanography, Faculty of Fisheries and Marine Science, Universitas Diponegoro, Jl. Prof. Jacob Rois Tembalang, Semarang, 50275, Indonesia

² Department of Naval Architecture, Ocean & Marine Engineering, Faculty of Engineering, University of Strathclyde, 16 Richmond Street, Glasgow, G1 1XQ, United Kingdom

³ Department of Industrial Technology, Vocational School Universitas Diponegoro, Jl. Prof. Jacob Rois Tembalang, Semarang, 50275, Indonesia

⁴ Director of Water and Air Police (Ditpolairud) Regional Police of Central Java, Jl. Yos Sudarso No. 57, Semarang, Central Java, 50174, Indonesia

* Corresponding author's e-mail: rikha.widiaratih@live.undip.ac.id

ABSTRACT

The real-time monitoring of ocean wave data is a crucial element in marine environmental monitoring and the development of marine resources. It is unfortunate that the majority of wave measurement devices remain challenging, relatively high-priced, and require sophisticated technology. This study investigates the validation of a new type of ocean wave measurement, designed based on the mini wave gauge (MWG), using low-cost materials. The study utilizes an accelerometer sensor, specifically the ADXL335, which is converted to measure wave height, and the GY-271 designed to measure wave direction. This research addresses the validation of MWG by comparing measurements from the acoustic doppler current profiler (ADCP) and HOBO. The validation of wave height demonstrates high accuracy, with a MAPE percentage of 0.46% between MWG and ADCP, and 23.30% between MWG and HOBO. In contrast, the validation of MWG for wave direction by ADCP still requires improvement, with a MAPE of 36.75%. This is due to the sensor's sensitivity to the earth's magnetic field, which requires further improvement of the buoy design to accommodate the direction of incoming waves. Additionally, the MWG's sampling rate in milliseconds allows for analyzing wave characteristics based on wave periods using the fast Fourier transform (FFT) method.

Keywords: marine monitoring, wave measurement, low-cost materials, accelerometer sensor, validation, Fourier transforms, wave characteristics.

INTRODUCTION

In the latest era, the practice of anonymous ocean exploration platforms has become a notable phenomenon, effectively transforming the conventional approach. It is spearheaded by the advancement of the internet of things (IoT) and artificial intelligence (AI), which have the potential to enhance ocean exploration and management capabilities (Valada et al., 2014; Yu et

al., 2013; Zhang et al., 2024). As a maritime nation with approximately 18.000 islands and the second longest coastline after Canada, Indonesia possesses considerable marine potential (Sui et al., 2020). It is of the utmost importance to implement a strategic plan that optimises the marine environment. This can be supported by real-time environmental and continuous monitoring data. One of the physical parameters of the sea that has an impact on the environment is

the data on ocean waves (Tandon et al., 2018). Ocean waves data are essential for a multitude of purposes, including coastal construction, coastal zonation, disaster mitigation, tourism, fishing, and the assessment of renewable energy potential (Behrens et al., 2024).

Nevertheless, the collection of data on ocean waves remains a challenging and costly endeavours. Most studies on wave data are based on wind data, which is then converted into ocean wave energy due to stress caused by wind (Shimura et al., 2022; Yevnin and Toledo, 2022). However, it should be considered that not all ocean waves are generated by wind, the remain can be generated from tidal phenomena, density, seismic activity, and other factors (Toffoli & Bitner-Gregersen, 2017). Currently, ocean wave data can be obtained from a variety of sources, including satellites (Quefeulou, 2004), ultrasonic sensors (Christensen et al., 2013), and acoustic Doppler current profilers (ADCPs) (Trenaman et al., 2002), light detecting and ranging (LIDAR) (Shiina, 2019), radio detection and ranging (RADAR) (Lyzenga, 2015), and numerous others.

This study is a continuous of the research conducted by Widiaratih et al. (2023), which focused on the development of a simple ocean wave measuring device, namely the mini wave gauge (MWG). The device was validated through ultrasonic measurements conducted in a laboratory setting. The preceding research validated the process through ultrasonics, which exhibited accuracy in measuring wave height in centimetres. However, this method proved unsuitable for measuring smaller waves, including capillary waves, ordinary gravity waves, infrared gravity waves, and others (Sorensen, 1993). This research aims to improve the validation of wave measurements in field experiment between the MWG to the acoustic doppler current profiler (ADCP) and the HOBO. HOBO is a brand of water level measuring device that is recorded from a pressure sensor.

In addition, this study employs the fast Fourier transfer (FFT) method to investigate the wave characteristics. The FFT method is utilized for wave decomposition from MWG and HOBO data recording, as it is a suitable approach for examining data with a high sampling rate in milliseconds, as obtained from the MWG and HOBO devices.

MATERIALS AND METHODS

Research location

This research project is concerned with the validation of the wave height data produced by the MWG system using two fabricated and ready-to-use measuring instruments, namely the ADCP and the HOBO. Each instrument has its own operational characteristics. Since the MWG data acquisition employs Wi-Fi, it is not appropriate for use over long distances. Instead, it can only be deployed in coastal areas with extensive coverage, typically within a radius of approximately 50 m. Furthermore, the power supply represents a significant challenge, limiting the duration for which data can be recorded. However, in this study, it is demonstrated that approximately two hours of data can be recorded. The field experiments conducted in shallow waters using ADCP and HOBO were carried out in different locations. Between the ADCP and MWG experiment was performed in Tambakrejo Waters, Semarang on November 10th, 2023, while the HOBO and MWG experiment was conducted in Teluk Awur Waters, Jepara on November 25th, 2023 (Figure 1).

Materials

The research employed three principal instruments for wave measurement: the mini wave gauge (MWG), the acoustic Doppler current profiler (ADCP), and the HOBO water data logger. The objective of this study is to validate the capacity of the MWG to quantify wave parameters, including wave height and direction. The MWG is a cost-effective instrument designed for wave measurement. The validation method involves a comparison of wave measurements obtained with the MWG and two other instruments: the ADCP type Sontek XR-750 kHz and the HOBO type U20L-04.

Wave measurement instruments

Mini wave gauge (MWG)

The MWG has been designed for the economical recording of wave height and direction data in real-time and continuously. The sampling rate for waves is approximately 0.1 seconds or 100 milliseconds, which makes it suitable for recording the types of small waves, such as capillary waves, ultra gravity waves, and ordinary gravity waves, that have wave periods of 0.1 seconds, 1

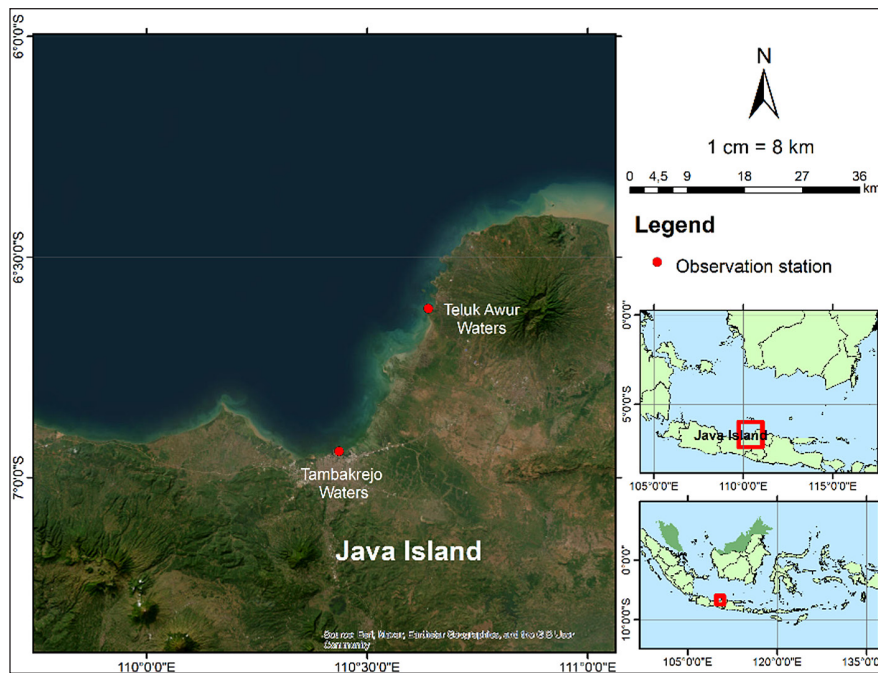


Figure 1. Research area in waters of the Tambakrejo Semarang (Mini Wave Gauge compared to ADCP, November 10th, 2023), and Teluk Awur Jepara (Mini Wave Gauge compared to HOBO, November 25th, 2023)

second, and 30 seconds, respectively (Sugizaki et al., 1993). The wave height is determined by an accelerometer (ADXL335), which gauges the discrepancy in elevation along the z-axis. The operational principle of the accelerometer hinges on the disparity in altitude along the z-axis (Earle and Bush, 1982). Moreover, the accelerometer is renowned for its high precision in determining accurate position (Qi et al., 2024). This exceptional capability of the accelerometer is leveraged to calculate the wave amplitude.

This accelerator is a widely utilized instrument for measuring vibrations across a multitude of parameters, including distance, speed, and numerous others (Zhao, 2010). Consequently, it is utilized in many aspects, including the study of earthquakes (Chen et al., 2023; Grover and Sharma, 2017; Huckfeldt et al., 2024), electron movement (Sharma et al., 2020), and the development of leakage detectors (Ismail et al., 2018), pedometer (Hao-ran et al., 2006), control movement by robotics (Vashisth et al., 2017), velocity in the river (Liu and Huang, 2021), and numerous other applications.

In this study, the ADXL335 accelerometer is employed to measure altitude differences, which are then converted to measure wave amplitude or wave height. Previous studies have utilized accelerometers designed appropriately for low frequencies (Gilbert, 1970). However, in this study,

an accelerometer with a newly developed sensor, which has not been previously used for wave measurement, specifically a sensor type ADXL335, which is suitable for a wide variety of frequencies, including high frequencies is applied.

The practicality of measuring waves using MWG is contingent upon its placement on the sea surface level. Once situated, the device will transmit real-time wave data via Wi-Fi to the user, who can access it through a laptop or computer. The block diagram and display of MWG are illustrated in Figure 2. It should be considered that the MWG is still in the process of development. However, the power supply used consists of four 7.4 V battery supply batteries, which presents a challenge for measurements over extended periods of time. Consequently, this study has been focused on validating the measurement of the height and direction of the sea wave against other fabricated wave instruments, such as ADCP and HOBO as water level logger.

Acoustic doppler current profiler (ADCP)

An ADCP is one of the qualified oceanography survey tools for measuring ocean currents and ocean waves (Trenaman et al., 2002). The ADCP utilized for validation is the Sontek XR-750 kHz, which employs acoustic waves to quantify wave height (Boufferrouk et al., 2016). The propagation

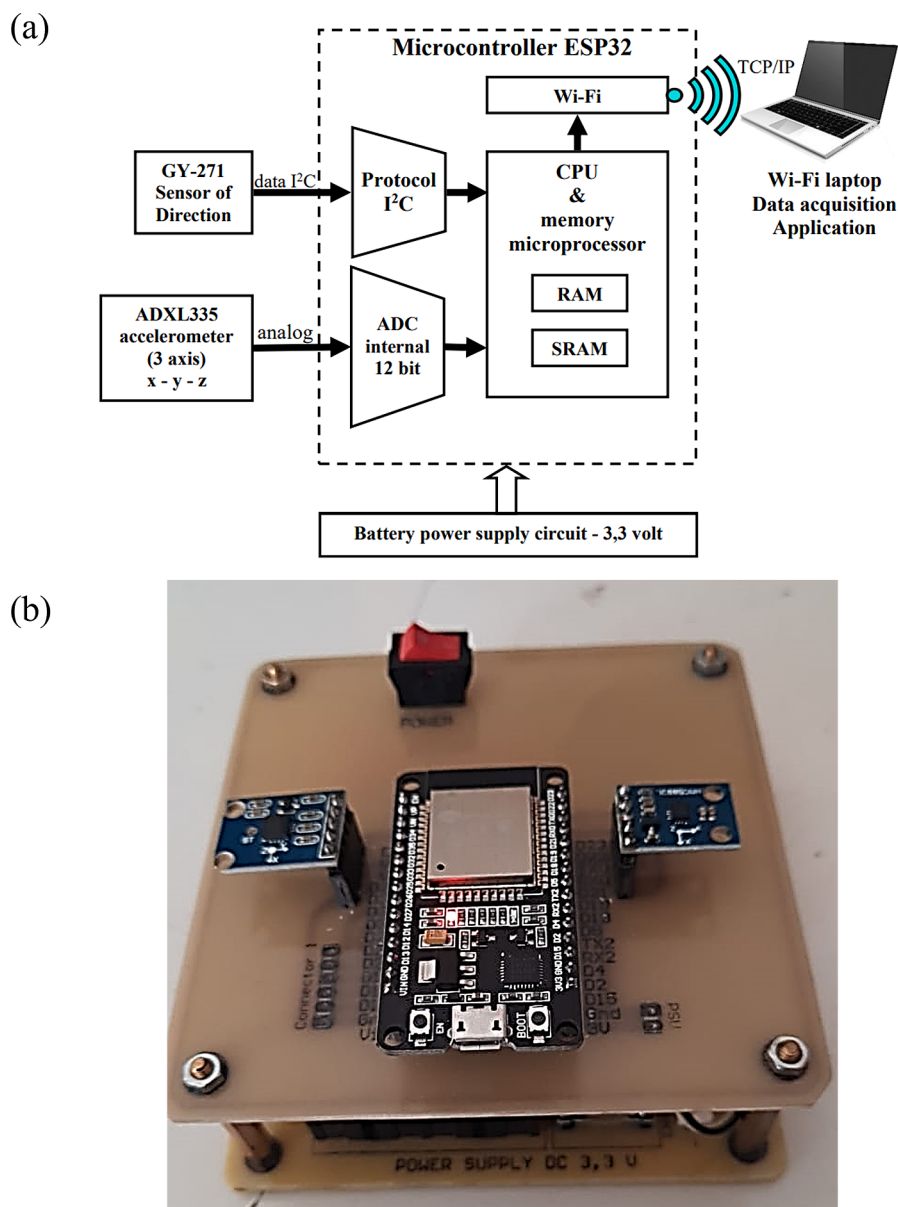


Figure 2. (a) Block diagram (a), and (b) display of mini wave gauge (Widiaratih et al., 2023)

of acoustic waves in the sea and the necessity for sophisticated technology to record data represent an advantage of this method. The ADCP utilized is the Sontek XR-750 kHz, which is capable of recording wave height and wave direction at a minimum of a 10-minute sampling rate (Dwinovantyo et al., 2017). Otherwise, the recording of small waves, such as capillary waves, ultra gravity waves, and ordinary gravity waves, would not be adequately captured (Hoitink et al., 2007).

Furthermore, the deployment of ADCP in field measurements may be situated on the seabed or mounted beneath the surface of the vessel (Shih et al., 2005). The validation of MWG with ADCP was conducted in the shallow waters of Tambakrejo, Semarang on November 10th, 2023,

between 16:00 and 18:00 Indonesian Western Indonesia Time (WIB). In this study, the ADCP was positioned on the seabed at a shallow depth. Additionally, the ADCP was lowered using a rope (Figure 3). Subsequently, the data were downloaded after the recording was complete.

HOBO

HOBO is one of a trademark of device utilized for the measurement of water levels or tidal in marine environments. It is positioned on the seabed for this purpose. The device is equipped with a pressure sensor, which is used to calculate the water level value. Prior studies have employed analogous instruments based on pressure



Figure 3. Implementation of acoustic doppler current profiler comparing wave measurement from mini wave gauge

sensors for the measurement of waves (Bishop & Donelan, 1987; Lyman et al., 2020). The validation of MWG data with HOBO was conducted on November 25th, 2023, at the Waters of Teluk Awur, Jepara, between the hours of 12:00 and 13:25 WIB. The specific HOBO device utilized was the U20L-04 water level logger, as illustrated in Figure 4. The data were acquired by downloading them directly from the HOBO device using a connector cable to a laptop or computer. It was necessary to implement a mechanism to extract the data pertaining to ocean waves from the water level collection data. The water level data were decomposed using the FFT to obtain the constituent waves. Subsequently, the tidal waves were distinguished, and the residual data were validated with data from MWG. Since the HOBO device has a higher sampling rate than the ADCP, resulting in a greater quantity of data.

Method

In general, the MWG configuration comprises four principal components such as the ESP32 microcontroller, the ADXL335 sensor, the GY-271

sensor for direction, and the circuit for supplying the data battery. The MWG is equipped with two principal sensors for the measurement of waves, namely the ADXL335 sensor, which serves as an accelerometer for the estimation of wave height. The accelerometer has three axes, namely x, y, and z. The difference in the z-axis is then converted into the height of the ocean waves (Shonting et al., 1996). The working principle of the accelerometer is to record the horizontal and vertical movements of the instrument (Elwany and Mahr, 2003).

Moreover, most methods for measuring wave direction typically employ ADCP, radar, and other sophisticated instruments (Dally, 2018). In this study, the MWG was equipped with a low-cost sensor utilising the GY-271, which is specifically designed for measuring wave direction. The operational principle of the GY-271 sensor is to ascertain the angular position and subsequently transform this into angular data (Mon, 2015). In addition, the two principal sensors for measuring waves are linked to the ESP32 microcontroller, which serves as the primary processing unit for data. The ESP32 microcontroller is equipped with



Figure 4. HOBO water level data logger type U20L-04

Wi-Fi, enabling further transmission of data to the user via a laptop or computer. To ensure a reliable power supply, the circuit employs four batteries each capacity 7.4 Volt.

Validation is employed to ascertain the extent of any errors, biases, and misalignments present in the sensor (Hassan and Bao, 2020). The calculation of deterministic errors in wave height and direction based on data recorded by MWG employs the MAE (Hodson, 2022), and the mean absolute percentage error (MAPE) (Rao & Shubhanga, 2018) with the formulas are represented in Equation 1 and 2, respectively.

$$MAE = \sum \frac{|y-y'|}{n} \tag{1}$$

$$MAPE = \frac{1}{n} \sum \left| \frac{y-y'}{y} \right| \times 100\% \tag{2}$$

where: *MAE* – mean absolute error; *MAPE* – mean absolute percentage error (%); *y* – actual data (ADCP; HOBO), *y'* – model data (MWG); *n* – quantity of data.

Moreover, the wave types were analyzed based on field measurement data obtained from the MWG and HOBO devices. The subsequent compilation of the wave data was then decomposed using the FFT. The FFT method is an effective tool for differentiating between various wave types based on their respective wave periods, ranging from ordinary gravity waves to trans-tidal waves (Adiningsih et al., 2022). Furthermore, the FFT allows for the decomposition of ocean wave types into various classifications, enabling the assessment of diverse types of data, including real-time recordings such as ultrasonic and acoustic, as well as radar images (Wei et al., 2016). By employing the wave decomposition mechanism, the distinctive characteristics of the

waves in the Tambakrejo and Teluk Awur waters can be identified.

RESULTS AND DISCUSSION

Validation mini wage gauge to acoustic doppler current profiler

The results of the data recording on the height and direction of waves from the MWG and ADCP in Tambakrejo Waters on November 10th, 2023, between the hours of 16:00 and 18:00 WIB, are presented in Figure 5. The ADCP type Sontek XR-750 kHz was constrained by a limited recording period of at least 10 minutes per sample, in a total recording duration of 2 hours, resulting in 12 data points, as illustrated in Figure 5. The time-sampling capability of an ADCP is dependent on its specifications. For instance, the 75-kHz Long Ranger ADCP can record data per 30 seconds, while the majority of wave-period exceeding one minute may be captured, smaller waves with periods of less than one minute may be excluded from the data set (Chang et al., 2011).

Furthermore, the result of the wave data recording by MWG in Tambakrejo Waters on November 10th, 2023, between 16:00 and 18:00 WIB, is illustrated in Figure 6. The wave height is represented by a black line, while the wave direction is indicated by a blue dot. The MWG sampling rate is 0.1 seconds (or 100 milliseconds), which allows for the generation of dense wave data and the capture of data from smaller waves.

The raw data from MWG, henceforth referred to as the data, was selected concurrently with the ADCP recording for the purposes of determining the wave height and direction, as illustrated in Figure 7.

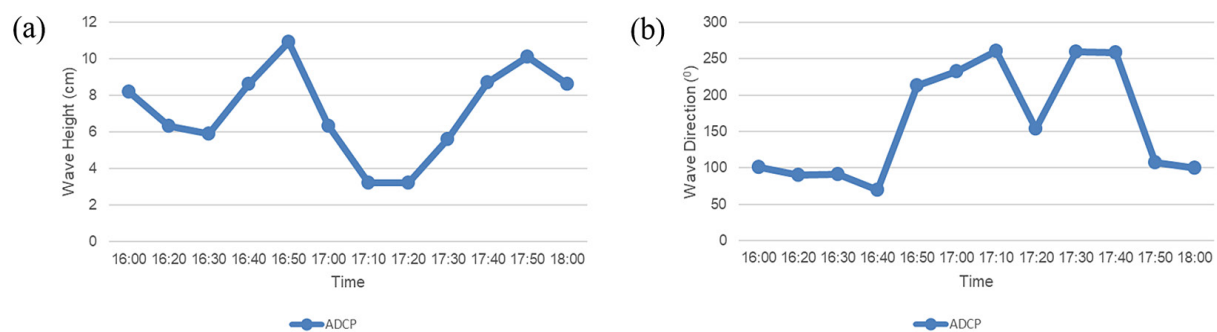


Figure 5. Wave measurement from acoustic doppler current profiler in Tambakrejo Waters, November 10th, 2023, 14:00–16:00 WIB (a) wave heights; and (b) wave direction

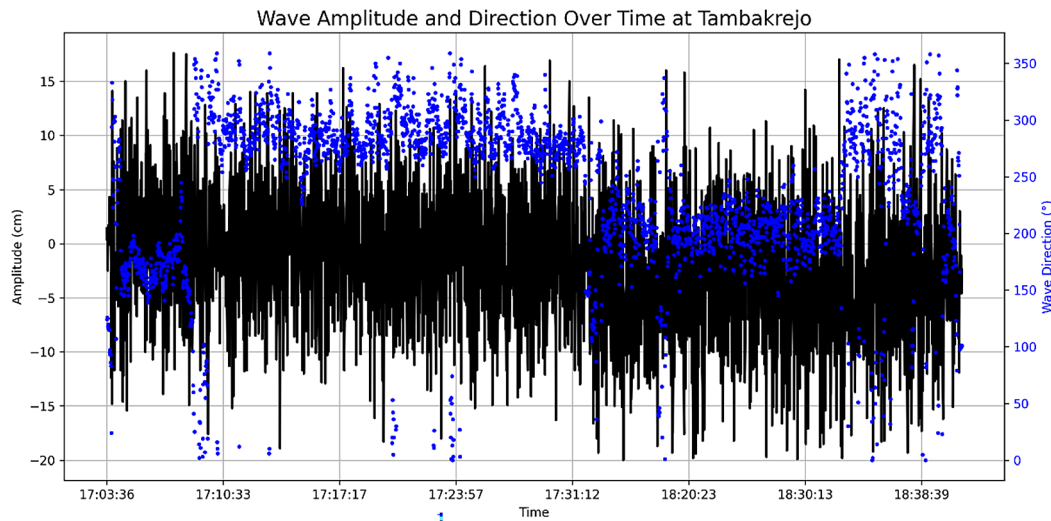


Figure 6. Wave measurement from mini wave gauge in Tambakrejo Waters, November 10th, 2023, 14:00–16:00 WIB, for wave heights (black), and wave direction (blue)

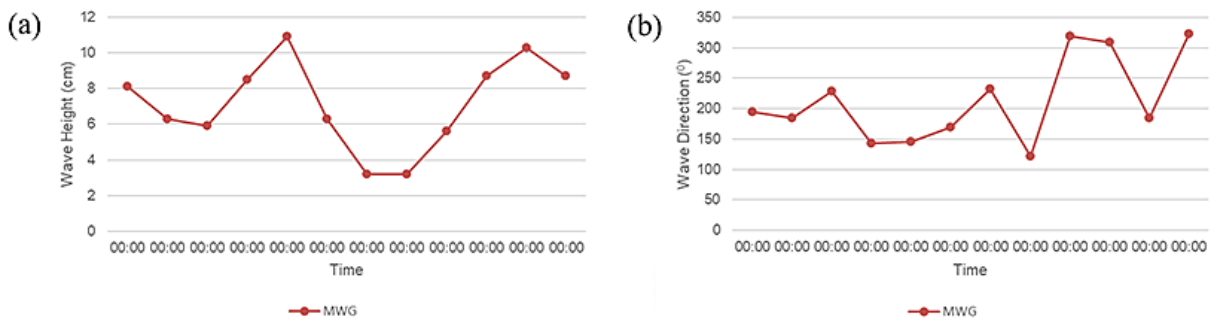


Figure 7. Wave measurement from mini wave gauge in Tambakrejo Waters, November 10th, 2023, with similar time with ADCP for (a) wave heights; and (b) wave direction

Moreover, the MWG data was subjected to a validation process in comparison with the ADCP data (Figure 8). The validation results between MWG and ADCP for wave height demonstrated a high degree of similarity in the values obtained, however there was still a need for improvement in the accuracy of the data for wave direction. The mean absolute error (MAE) and the mean absolute percentage error (MAPE) calculations yielded values of 0.04 cm and 0.46% for wave height, respectively, while for wave direction, the values reached 83.3° and 36.76%. The present experiment demonstrates the performance of the MWG in measuring wave properties, specifically wave height and direction. The MWG, which is equipped with the accelerometer ADXL335, exhibited high accuracy and suitability for measuring wave height. This is supported by the fact that the ADXL335 can detect small movements with precision down to the millimeter (Ma et al., 2025).

Nevertheless, the wave direction source from sensor GY-271 still exhibits a lack of accuracy. The sensor was designed to record the angular position; however, field experiments revealed a lack of precision due to a drifting phenomenon that resulted in a discrepancy between actual conditions and sensor readings (Mangkusasmito et al., 2020). Furthermore, the design of the MWG buoy was found to contribute to drift, as it was unable to accommodate the direction of wave arrival. As a result, modifications to the MWG buoy design are necessary for future studies. Additionally, the error in wave direction can be improved by implementing a filter in the algorithm (Bachtiar et al., 2023).

Validation mini wave gauge to HOB0

The validation of wave measurements obtained using MWG in comparison to ADCP

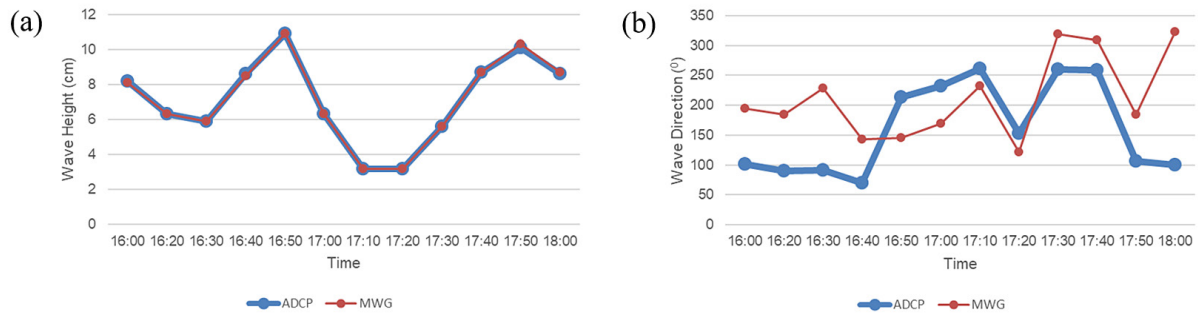


Figure 8. Comparison of wave height (left) and wave direction (right) between mini wave gauge (red) and ADCP (blue)

demonstrated excellent performance. However, due to the limited availability of wave data from ADCP, it was necessary to employ an additional instrument capable of providing compact wave data for validation purposes. Moreover, the wave data from MWG were validated against data from HOBO, which is a water level measuring instrument. Although HOBO is primarily utilized as a water level logger, it can be employed for wave validation through the decomposition of wave constituents, which include tidal, wind, density, and other factors. The validation of MWG to HOBO wave data was limited to a comparison of available wave height, as the wave direction was not applicable since HOBO was unable to record this data. The raw data from HOBO (black) and MWG (blue) in the Waters of Teluk Awur Jepara on

November 25th, 2023, between 12:00 and 13:25 WIB, is shown in Figure 9.

Generally, water level data has a similar pattern with tidal data, as appointed main function of HOBO. To obtain wave data from water level data, additional processes were required to decompose the water level data into its constituent components using the FFT. Furthermore, the water level data was distinguished from the tidal wave data, and the residual waves data were retained. These residual waves are subsequently compared to MWG data, as illustrated in Figure 10. There were differences in the time sampling rate of MWG and HOBO, which were 0.1 seconds and 1 second, respectively. Consequently, the MWG data followed the amount and sampling rate of HOBO data. Given that the sampling rate was in seconds, it was possible to

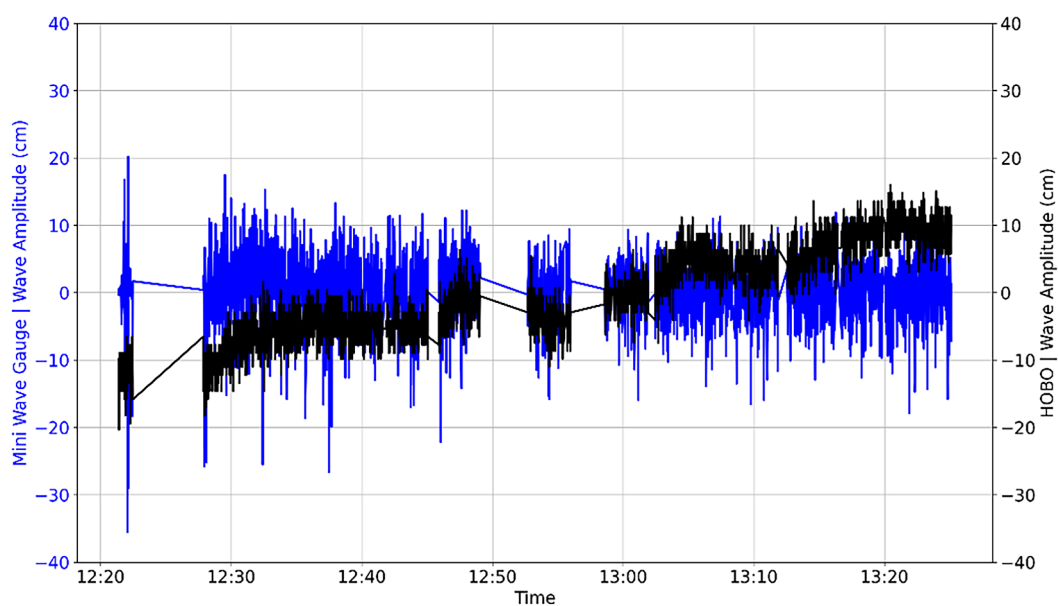


Figure 9. Wave measurement from mini wave gauge n Teluk Awur Waters, November 25th, 2023, 12:00–13:25 WIB for HOBO (black), and mini wave gauge (blue)

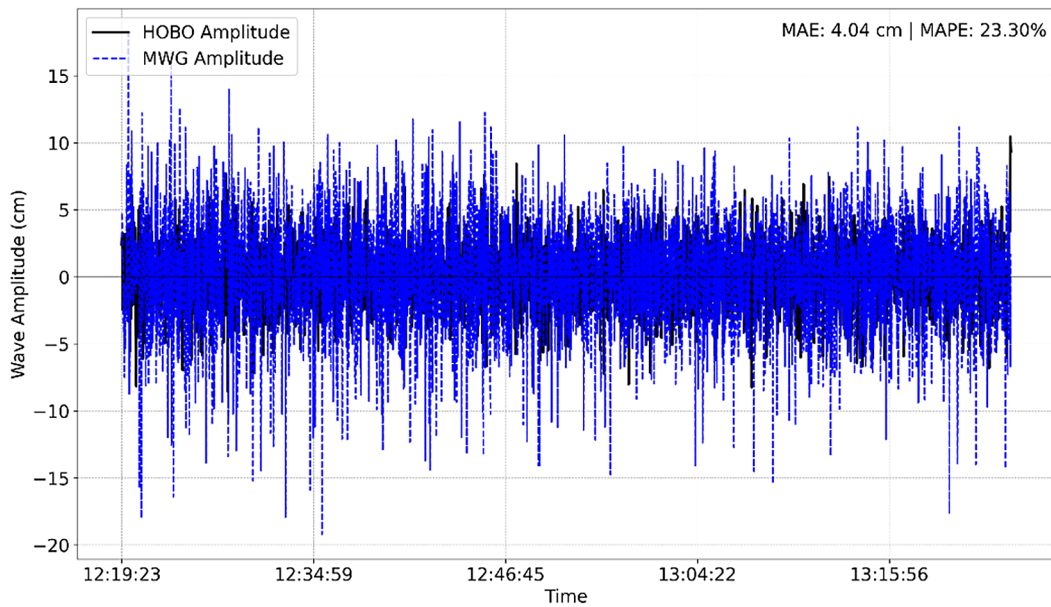


Figure 10. Comparison of wave height between HOBO (black) and mini wave gauge (blue)

capture the small wave periods that were visible in the rapid fluctuating pattern.

The validation of wave height measurements obtained using the MWG device demonstrated a high degree of correlation with data obtained from the HOBO instrument. The error estimation employed the MAE and the mean percentage error (MAPE) from MWG to HOBO, yielding values of 4.04 cm and 23.30%, respectively. The level error is higher than that achieved by ADCP, which operates on the principle of the HOBO device, which is based on a pressure sensor and subsequently converts the data to water level information. Even though previous studies have employed HOBO for wave measurements, it has been demonstrated to be more appropriate for long wave periods, such as sea and swell, than for small waves (Risandi et al., 2022). Furthermore, the occurrence of bias issues can be associated to the dynamics of the relative motion effect, which is sourced from water particles and is predominantly observed in surface water (Cavaleri, 1980).

Overall, the MWG exhibits high accuracy comparable to that of commercial instruments

such as ADCP and HOBO during field tests, as illustrated in Table 1. The accuracy test of wave height is higher than that of wave direction. The latter is influenced by the sensors selected, whereas the accelerator of ADXL 335 is suitable for various applications requiring precise measurements. Furthermore, it has high sensitivity to various movements and is compatible with a large range of frequencies (Ma et al., 2025). In the case of wave direction, however, further processing is necessary to account for the influence of the Earth’s magnetic field, which can be addressed using algorithms or the optimization of the buoy design (Barstow et al., 1991; Steele, 2003).

Wave characteristic based on wave decomposing using FFT

The characteristics of waves are of high importance in the planning of coastal areas, particularly in the case of the waters in Tambakrejo and Teluk Awur. Since, in these areas are used extensively by productive zones, including ports, settlements, industrial areas, fishponds

Table 1. Validation of MWG to ADCP and HOBO based on MAE and MAPE

Error measurement	Wave height		Wave direction	
	MAE (cm)	MAPE (%)	MAE (°)	MAPE (%)
MWG vs ADCP	0.04	0.46	83.36	36.76
MWG vs HOBO	4.04	23.30	N/A	N/A

and others. The characteristics of waves can be obtained by wave decomposition using the FFT method. This demonstrates that frequency domain approaches are more effective than time domain methods in identifying the characteristics of waves (De-gan et al., 2000).

In general, the various types of waves can be classified into seven categories based on their respective periods. These include capillary waves (0.1 seconds), ultra gravity waves (1 second),

ordinary gravity waves (30 seconds), infra gravity waves (5 minutes), and ordinary tides waves (12–24 hours). The results of the FFT decomposition of the data from Tambakrejo Waters on November 10th, 2023, between 16:00 and 18:00 (WIB), have identified three distinct wave types: ordinary gravity waves, infra-gravity waves, and long-period waves (Figure 11).

Moreover, the wave characteristics observed in Teluk Awur Waters, derived from

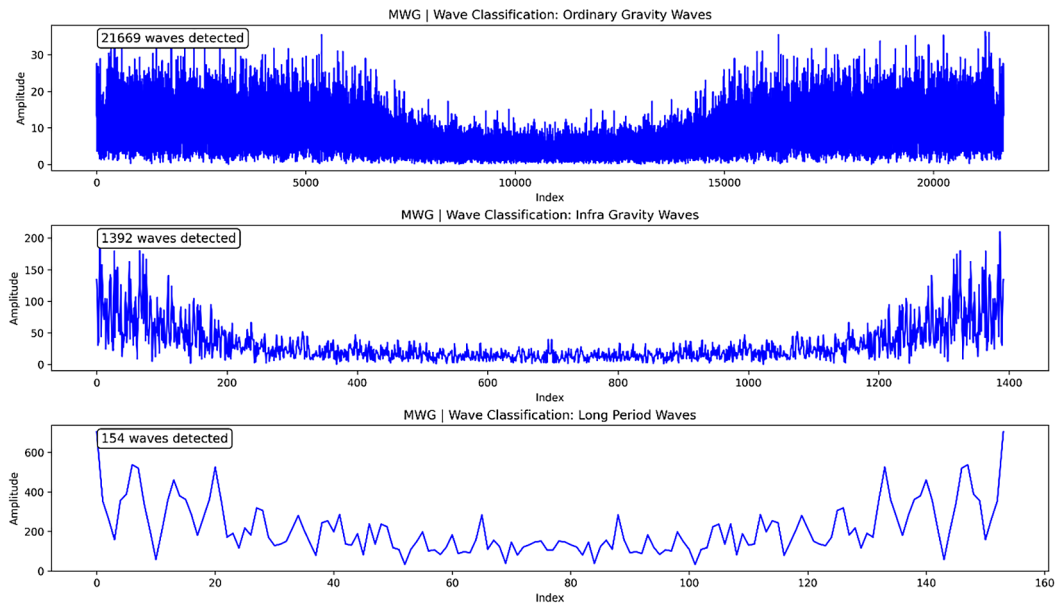


Figure 11. Wave decomposition from mini wave gauge (MWG) using fast fourier transform (FFT) in Tambakrejo Waters, November 10th, 2023, 16:00–18:00 WIB

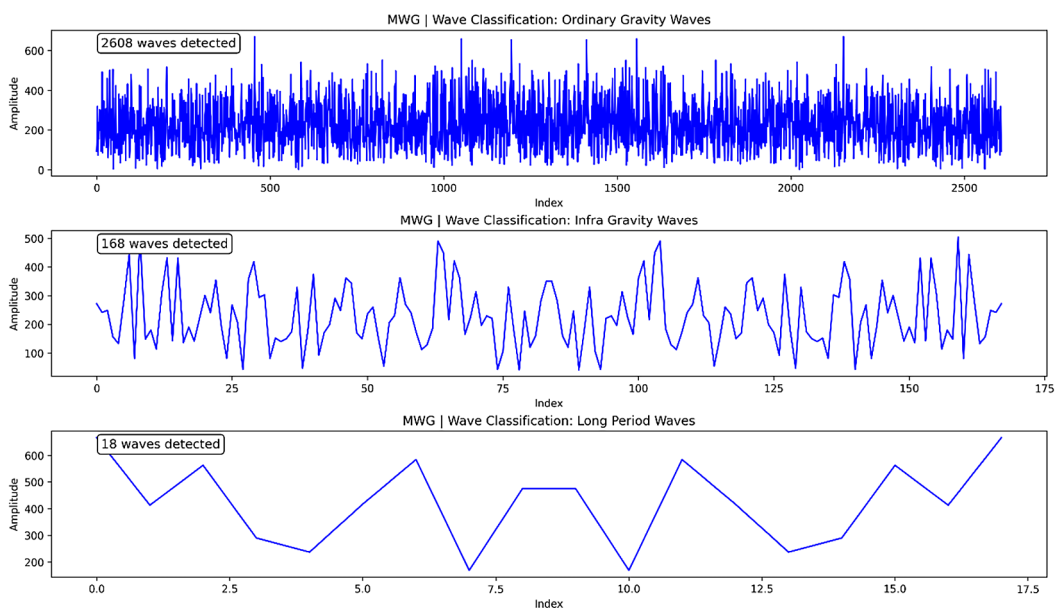


Figure 12. Wave decomposition from mini wave gauge using fast fourier transform in Teluk Awur Waters, November 25th, 2023, 12:00–13:25 WIB

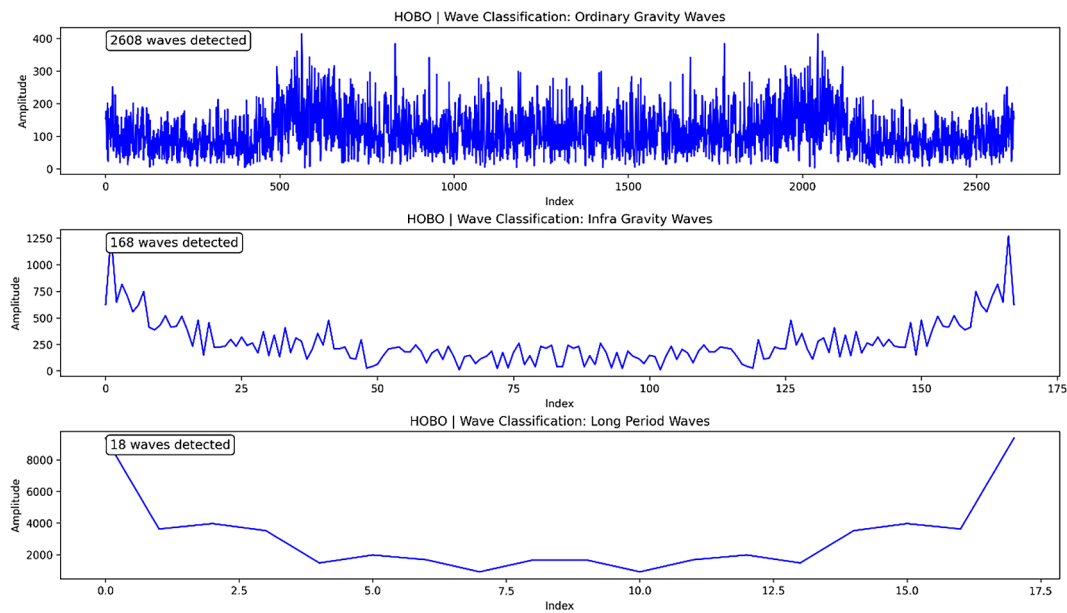


Figure 13. Wave decomposition from HOBO using fast Fourier transform (FFT) in Teluk Awur Waters, November 25th, 2023, 12:00–13:25 WIB

MWG and HOBO data, are illustrated in Figures 12 and 13, respectively. The wave characteristics observed in Teluk Awur Waters exhibited a comparable pattern to those observed in Tambakrejo Waters, with the emergence of three distinct types of waves. In both the Waters of Tambakrejo and Teluk Awur, ordinary gravity waves were identified as the most dominant type of wave. These waves were found to be induced by a range of activities, including gravity, inertia, wind, shipping, and coastal buildings (Dhanak and Xiros, 2016). Additionally, the pattern of wave decompositions sourced from HOBO exhibited a resemblance to tidal waves generally.

CONCLUSIONS

The accuracy of the MWG for measuring wave height and direction has been demonstrated through a process of validation. This has involved a comparison with the ADCP and HOBO instruments, which have been shown to provide comparable results. The deployment of the MWG presents a potential tool for the broader utilisation of cost-effective instrumentation for wave measurement, with indications of efficacy in efficient data acquisition and the use of low-cost materials. Furthermore, the accelerometer ADXL335 demonstrates excellent fidelity in

real-time wave height measurement due to its sensitivity to minute movements. However, the wave direction indicated by the GY-271 sensor exhibits a tendency towards bias, and thus remains a subject of ongoing development. In future studies, it would be beneficial to apply the aforementioned validation in long-term measurements. Additionally, parameters such as battery life and data acquisition via internet connection should be considered. Furthermore, the buoy design should be given due attention to prevent leakage and to allow for a more optimal direction of the incoming wave.

Acknowledgments

This research was conducted as part of the International Publication Research (RPI) program, sponsored by the Institution of Research and Community Service (LPPM) at the University of Diponegoro. The funding for this research was provided by: In addition to APBN funding from Universitas Diponegoro for the 2023 financial year, the authors would like to express their gratitude to all those who have provided financial support for this research project. This research project has been undertaken in accordance with the decision of the Institutional Research and Community Service of Universitas Diponegoro, as set forth in Activity Assignment Letter Number 609-58/UN7.D2/PP/VIII/2023.

REFERENCES

- Adiningsih, S., Fadlilah, Y. N., Putranto, R. T., Agfanita, S., Bayrus, S., Iriani, R. N., Wicaksono, M., Ikhtiarino, S., Wulandari, S., Adyaksa, Y., Petrova, C. B., Ginanjar, S., Wirasatriya, A., Widiaratih, R., Sugianto, D. N., Kunarso, K., Susanto, R. D. (2022). An FFT-Based Method for Wave Decomposition from Wave and Tide Monitoring Using A01NYUB Sensor. *Proceeding - 2022 IEEE Ocean Engineering Technology and Innovation Conference: Management and Conservation for Sustainable and Resilient Marine and Coastal Resources, OETIC*, 30–37. <https://doi.org/10.1109/OETIC57156.2022.10176211>
- Barstow, S. F., Ueland, G., Krogstad, H. E., Fossum, B. A. (1991). The Wavescan second generation directional wave buoy. *IEEE Journal of Oceanic Engineering*, 16(3), 254–266. <https://doi.org/10.1109/48.90882>
- Behrens, J., Olfe, C., Cameron, G., Bucciarelli, R., Timmerman, R., Wright, D., Lodise, J., Merrifield, S., Terrill, E. (2024). Coastal data information program: advances in measuring and modeling wave activity, climate, and extremes. *Coastal Engineering Journal*, 66(1), 3–16. <https://doi.org/10.1080/21664250.2024.2308021>
- Bishop, C. T., & Donelan, M. A. (1987). Measuring waves with pressure transducers. *Coastal Engineering*, 11(4), 309–328. [https://doi.org/10.1016/0378-3839\(87\)90031-7](https://doi.org/10.1016/0378-3839(87)90031-7)
- Bouferrouk, A., Saulnier, J.-B., Smith, George. H., Johanning, L. (2016). Field measurements of surface waves using a 5-beam ADCP. *Ocean Engineering*, 112, 173–184. <https://doi.org/10.1016/j.oceaneng.2015.12.025>
- Cavaleri, L. (1980). Wave measurement using pressure transducer. *Oceanologica Acta*, 3, 339–346. <https://api.semanticscholar.org/CorpusID:67825798>
- Chang, M. H., Lien, R. C., Yang, Y. J., Tang, T. Y. (2011). Nonlinear internal wave properties estimated with moored ADCP measurements. *Journal of Atmospheric and Oceanic Technology*, 28(6), 802–815. <https://doi.org/10.1175/2010JTECHO814.1>
- Chen, F. H., Shieh, H. L., Tu, J. F. (2023). Development of earthquake detection and warning system based on sensors. *Sensors and Materials*, 35(4), 1211–1220. <https://doi.org/10.18494/SAM4116>
- Christensen, K. H., Röhrs, J., Ward, B., Fer, I., Broström, G., Saetra, Ø., Breivik, Ø. (2013). Surface wave measurements using a ship-mounted ultrasonic altimeter. *Methods in Oceanography*, 6, 1–15. <https://doi.org/10.1016/j.mio.2013.07.002>
- Dally, W. R. (2018). Comparison of a mid-shelf wave hindcast to ADCP-measured directional spectra and their transformation to shallow water. *Coastal Engineering*, 131, 12–30. <https://doi.org/10.1016/j.coastaleng.2017.10.009>
- De-gan, Z., Hao, X., Gao, G., Zhao, H. (2000). A method of FFT-based wavelet transform. *Journal of Northeastern University*, 21(6), 599–601.
- Dhanak, M. R., & Xiros, N. I. (2016). Springer Handbook of Ocean Engineering. <https://doi.org/10.1007/978-3-319-16649-0>
- Dwinovantyo, A., Manik, H. M., Prartono, T., Susilohadi, S. (2017). Quantification and analysis of suspended sediments concentration using mobile and static acoustic doppler current profiler instruments. *Advances in Acoustics and Vibration*. <https://doi.org/10.1155/2017/4890421>
- Earle, M., & Bush, K. (1982). Strapped-down accelerometer effects on NDBO wave measurements. *OCEANS* 82, 838–848. <https://doi.org/10.1109/OCEANS.1982.1151908>
- Elwany, H., & Mahr, R. (2003). Deep water directional wave measurements from pressure, wave velocities and a three-axis accelerometer. *Proceedings of the IEEE/OES Seventh Working Conference on Current Measurement Technology*, 127–127. <https://doi.org/10.1109/CCM.2003.1194298>
- Gilbert, R. L. G. (1970). The Bedford institute wave recorder. *Journal of Geophysical Research*, 75(27), 5215–5224. <https://doi.org/10.1029/JC075i027p05215>
- Grover, V., & Sharma, A. (2017). Prediction of earthquake using 3 axis accelerometer sensor (ADXL335) and ARDUINO UNO. *International Journal of Science and Research (IJSR)*, 6(9), 1044–1047.
- Hao-ran, S., Wenshuai, L., Yiming, Z. (2006). Using 3-Axis Accelerometer ADXL330 to High Accuracy Pedometer. *Chinese Journal of Sensors and Actuators*, 19(4).
- Hassan, M. ul, & Bao, Q. (2020). A Field Calibration Method for Low-Cost MEMS Accelerometer Based on the Generalized Nonlinear Least Square Method. *Multiscale Science and Engineering*, 2(2–3), 135–142. <https://doi.org/10.1007/s42493-020-00045-2>
- Hodson, T. O. (2022). Root-mean-square error (RMSE) or mean absolute error (MAE): when to use them or not. *Geoscientific Model Development*, 15(14), 5481–5487. <https://doi.org/10.5194/gmd-15-5481-2022>
- Hoitink, A. J. F., Peters, H. C., Schroevers, M. (2007). Field verification of ADCP surface gravity wave elevation spectra. *Journal of Atmospheric and Oceanic Technology*, 24(5), 912–922. <https://doi.org/10.1175/JTECH2000.1>
- Huckfeldt, M., Wöske, F., Rievers, B., List, M. (2024). GRACE Follow-On accelerometer data recovery by high-precision environment modelling.

- Advances in Space Research*, 73(12), 5783–5805. <https://doi.org/10.1016/j.asr.2024.03.068>
23. Liu, W. C., & Huang, W. C. (2021). Development of a three-axis accelerometer and large-scale particle image velocimetry (LSPIV) to enhance surface velocity measurements in rivers. *Computers and Geosciences*, 155. <https://doi.org/10.1016/j.cageo.2021.104866>
 24. Lyman, T. P., Elsmore, K., Gaylord, B., Byrnes, J. E. K., Miller, L. P. (2020). Open wave height logger: An open source pressure sensor data logger for wave measurement. *Limnology and Oceanography: Methods*, 18(7), 335–345. <https://doi.org/10.1002/lom3.10370>
 25. Lyzenga, D. R. (2015). *Real-time estimation of ocean wave fields from marine radar data*. IGARSS : 2015 IEEE International Geoscience & Remote Sensing Symposium : Proceedings : July 26–31, Milan, Italy, 3622–3625.
 26. Ma, Z., Choi, J., Lee, J., Sohn, H. (2025). Accelerometer-aided millimeter-wave radar interferometry for uninterrupted bridge displacement estimation considering intermittent radar target occlusion. *Mechanical Systems and Signal Processing*, 223. <https://doi.org/10.1016/j.ymsp.2024.111888>
 27. Mangkusamito, F., Tadeus, D. Y., Winarno, H., Winarno, E. (2020). Accuracy improvement of gy-521 mpu-6050 sensor with drift factor correction method. *Ultima Computing : Jurnal Sistem Komputer*, 12(2), 91–95. <https://doi.org/10.31937/sk.v12i2.1791> (In Bahasa).
 28. Bachtiar, M. M., Wibowo, I. K., Rifa’I, Y., Subagja, D. P., Syahriyah, N. A. (2023). Estimation of axis roll pitch of GY-91 IMU sensor reading using kalman filter. *International Journal of Artificial Intelligence & Robotics (IJAIR)*, 5(2), 63–70. <https://doi.org/10.25139/ijair.v5i2.7179>
 29. Ismail, M. I. M., Dziauddin, R. A., Salleh, N. A. M., Ahmad, R., Azmi, M. H.B., Kaidi, H. M. (2018). *Analysis and procedures for water pipeline leakage using three-axis accelerometer sensors: ADXL335 and MMA7361*. IEEE Access, 6, 71249–71261. <https://doi.org/10.1109/ACCESS.2018.2878862>
 30. Mon, Y.-J. (2015). The gyroscope sensor test by using Arduino platform. *International Journal of Scientific & Technology Research*, 4, 398–400.
 31. Qi, F., Chen, G., Zhao, X., Wang, X. (2024). A high-precision positioning method for shield tunneling based on dual-axis hybrid inertial navigation system. Measurement: *Journal of the International Measurement Confederation*, 224. <https://doi.org/10.1016/j.measurement.2023.113915>
 32. Quefeulou, P. 2004. Long-term validation of wave height measurements from altimeters. *Marine Geodesy*, 27(3–4), 495–510. <https://doi.org/10.1080/01490410490883478>
 33. Rao, K., & Shubhanga, K. N. 2018. MAPE - an alternative fitness metric for prony analysis of power system signals. *International Journal of Emerging Electric Power Systems*, 19(6). <https://doi.org/10.1515/ijeeps-2018-0091>
 34. Risandi, J., Solihuddin, T., Kepel, T. L., Daulat, A., Heriati, A., Mustikasari, E., Hidayat, R. (2022). Low-cost investigation of wave dynamics across low energy reef environments in Indonesia. *IOP Conference Series: Earth and Environmental Science*, 1119(1). <https://doi.org/10.1088/1755-1315/1119/1/012033>
 35. Sharma, R., Kumar, P., Ojha, S., Gargari, S., Chopra, S. (2020). Inter-university accelerator centre, New Delhi (IUACD) radiocarbon date list I. *Radiocarbon*, 62(5), e1–e13. <https://doi.org/10.1017/RDC.2020.44>
 36. Shih, H. H., Long, C., Bushnell, M., Hathaway, K. (2005). Intercomparison of Wave Data Between Triaxys Directional Wave Buoy, ADCP, and Other Reference Wave Instruments. *24th International Conference on Offshore Mechanics and Arctic Engineering*, 2, 655–663. <https://doi.org/10.1115/OMAE2005-67235>
 37. Shiina, T. (2019). *Sea wave dynamics visualization and its interaction with the surface atmosphere by LED mini-lidar*. In C. R. Bostater, X. Neyt, & F. Viallefont-Robinet (Eds.), *Remote Sensing of the Ocean, Sea Ice, Coastal Waters, and Large Water Regions*, 11150, 21. SPIE. <https://doi.org/10.1117/12.2533406>
 38. Shimura, T., Mori, N., Baba, Y., Miyashita, T. (2022). Ocean surface wind estimation from waves based on small GPS buoy observations in a bay and the open ocean. *Journal of Geophysical Research: Oceans*, 127(9). <https://doi.org/10.1029/2022JC018786>
 39. Shonting, D., Middleton, F., Knox, J., Hebda, P. (1996). A submarine-launched wave measuring buoy. *Ocean Engineering*, 23(6), 465–481. [https://doi.org/10.1016/0029-8018\(95\)00055-0](https://doi.org/10.1016/0029-8018(95)00055-0)
 40. Sorensen, R. M. (1993). Basic wave mechanics: for coastal and ocean engineers. *A Wiley-Interscience Publication, John Wiley & Sons*. 304.
 41. Steele, K. E. (2003). Pitch-roll buoy mean wave directions from heave acceleration, bow magnetism, and starboard magnetism. *Ocean Engineering*, 30(17), 2179–2199. [https://doi.org/10.1016/S0029-8018\(03\)00082-9](https://doi.org/10.1016/S0029-8018(03)00082-9)
 42. Sugizaki, G., Takenaka, T., Toda, K. (1993). Motion characteristics measurement of rotating object using surface acoustic wave oscillator. *Japanese Journal of Applied Physics*, 32, 4237. <https://doi.org/10.1143/JJAP.32.4237>
 43. Sui, L., Wang, J., Yang, X., Wang, Z. (2020). Spatial-temporal characteristics of coastline changes in Indonesia from 1990 to 2018. *Sustainability*, 12(8). <https://doi.org/10.3390/su12083242>

44. Tandon, A., Venkatesan, R., D'Asaro, E., Atmanand, M. (2018). *Observing the Oceans in Real Time*. (Eds.), <https://doi.org/10.1007/978-3-319-66493-4>, 323 Springer pub., <http://www.springer.com/us/book/9783319664927>. <https://doi.org/10.1007/978-3-319-66493-4>
45. Toffoli, A., & Bitner-Gregersen, E. M. (2017). *Types of ocean surface waves, wave classification*. In *Encyclopedia of Maritime and Offshore Engineering*, 1–8. Wiley. <https://doi.org/10.1002/9781118476406.emoe077>
46. Trenaman, N., Devine, P., Strong, B. (2002). ADCP-based multidirectional wave gauge and current profiling. *Oceans '02 MTS/IEEE*, 1763–1766. <https://doi.org/10.1109/OCEANS.2002.1191900>
47. Valada, A., Velagapudi, P., Kannan, B., Tomaszewski, C., Kantor, G., Scerri, P. (2014). Development of a low cost multi-robot autonomous marine surface platform. *Springer Tracts in Advanced Robotics*, 92, 643–658. https://doi.org/10.1007/978-3-642-40686-7_43
48. Vashisth, R., Sharma, A., Malhotra, S., Deswal, S., Budhraj, A. (2017). Gesture Control Robot Using Accelerometer. *ISPCC 2017 : 4th IEEE International Conference on Signal Processing, Computing and Control* : September 21–23, 150–153.
49. Wei, Y., Lu, Z., Zhang, J.-K. (2016). A novel method to retrieve sea wave components from radar image sequence. *2016 IEEE International Conference on Mechatronics and Automation*, 1691–1696. <https://doi.org/10.1109/ICMA.2016.7558818>
50. Widiaratih, R., Suryoputra, A. A. D., Handoyo, G., Satriadi, A., Putranto, A. B. (2023). Prototype of simple mini-wave gauge using Microcontroller ESP32 on the laboratory scale. *IOP Conference Series: Earth and Environmental Science*, 1224(1). <https://doi.org/10.1088/1755-1315/1224/1/012024>
51. Yevnin, Y., & Toledo, Y. (2022). *A Deep Learning Model for Improved Wind and Consequent Wave Forecasts*. <https://doi.org/10.1175/JPO-D-21>
52. Yu, Y., Gu, L., Wu, X. (2013). The Application of Artificial Intelligence in Ocean Development. *Advanced Materials Research*, 864–867, 2116–2119. <https://doi.org/10.4028/www.scientific.net/AMR.864-867.2116>
53. Zhang, A., Wang, W., Bi, W., Huang, Z. (2024). A path planning method based on deep reinforcement learning for AUV in complex marine environment. *Ocean Engineering*, 313, 119354. <https://doi.org/10.1016/j.oceaneng.2024.119354>
54. Zhao, N. (2010). Full-featured pedometer design realized with 3-Axis digital accelerometer. *Analog Dialogue*, 44(6).